# Hopping transport in δ-doping layers in GaAs

Qiu-yi Ye, B. I. Shklovskii,* A. Zrenner, and F. Koch
*Physik-Department (E16), Technische Universität München, D-8046 Garching bei München, Federal Republic of Germany*

K. Ploog
*Max-Planck-Institut für Festkörperforschung, Postfach 80 06 65, D-7000 Stuttgart 80, Federal Republic of Germany*
(Received 9 June 1989; revised manuscript received 4 December 1989)

We consider hopping transport in a dilutely doped sheet of Si donors in GaAs. Samples are constructed as multiple δ layers, spaced significantly farther apart than the average, in-plane donor separation. In this system we have determined activation energies and studied the positive magnetoresistance effect quantitatively. We provide a detailed examination of the negative-magnetoresistance effect that stems from quantum interference of neighboring hopping paths.

## I. INTRODUCTION

Electronic transport in doped semiconductors has been studied in a wide range of temperatures and density of dopant atoms. It is truly a classic subject in three-dimensional, bulk semiconductor physics encompassing many different modes of transport. At sufficiently low temperature and dopant concentration, the dominant mode of conduction is carrier hopping from occupied to unoccupied localized impurity states. Hopping transport is described extensively in the literature.[1]

It has been recognized that the hopping mode of transport can also be observed in the low-dimensional semiconductor systems. In particular, Fowler and co-workers[2] have dedicated a great deal of effort to experiments on metal-oxide-semiconductor (MOS) channel transport. In these experiments, a number of positively charged ions ($N_{ox}$) can be drifted to the $Si/SiO_2$ interface to provide the randomly positioned, ionic impurity potentials for channel electrons. The electron density $N_s$, in effect the degree of compensation in such a system, can be varied continuously using the gate voltage to sweep $N_s$ from below $N_{ox}$ to above this value. More recently, Robert and co-workers[3] have dealt with transport in remotely doped $GaAs/Al_xGa_{1-x}As$ heterostructures. In this two-dimensional (2D) system, electrons in the GaAs bind to the Si-dopant ion positioned near the interface in the $Al_xGa_{1-x}As$. In both the drifted-ion and doped heterostructure experiments, the scatter in the position of the ions relative to the interface, and thus relative to the location of the electrons, gives disorder in the strength of the Coulombic potentials. In addition, surface roughness in these systems will influence the electron binding.

Given the techniques of deliberate and controlled layered epitaxial growth, it has become possible to create an atomically sharp, confined layer of dopant atoms. The so-called δ-doping layer of Si donors in molecular-beam-epitaxy (MBE)-grown GaAs has been introduced in Ref. 4 and investigated in great detail since then.[5–8] It has been recognized that such layers are nearly ideal systems on which to investigate 2D hopping transport and localization-related effects.[8,9] The layers are characterized with the usual precision of MBE growth. The ionic position relative to the plane in which the electron moves is well known.

There is current interest in the negative-magnetoresistance (MR) effect in variable-range hopping. Nguyen *et al.*,[10] and more recently Sivan *et al.*,[11] point out that the interference of different hopping paths between initial and final states leads to negative MR. Such an effect, although very small, was first mentioned for experimental work on Si MOS channel transport with $Na^+$-contaminated interfaces.[12] In a more extensive publication[2] on the same MOS system, no further reference is made to the negative MR. The negative MR effect is observed for thin films of vapor-deposited $In_2O_3$ (Ref. 13) and in a depleted metal-semiconductor field-effect transistor (MESFET) structure.[14] We have observed the effect clearly in δ-layer transport.[9] Stimulated by these results, Schirmacher[15] has devised a theory based on interfering paths, arranged as a triangle in the sample plane. This theory provides a good description for the experiments.

The present work reports on hopping transport and magnetoresistance in a dilute δ-doped multilayer system. Transport measurements provide rich data for the fundamental study of strong localization effects. The δ layer is a simple and well-characterized 2D system. It is ideal for a quantitative comparison with theory. The δ layer is, in some respects, similar to the Ge grain-boundary layers for which hopping transport has been studied.[16] By contrast, the carrier density is more easily controlled and *n*-type donor layers are obtained for the GaAs δ system.

Section II gives details of the sample construction and describes the measurement techniques. Section III contains the experimental results together with a discussion of current theoretical ideas. Section IV summarizes what has been achieved.

## II. EXPERIMENTAL NOTES: DESIGN OF THE MULTI δ-LAYER SAMPLES

The GaAs amples investigated here are grown by molecular-beam epitaxy according to the stop-and-go

 

growth procedure introduced in Ref. 7. The Si donors are introduced in calibrated, controlled quantity onto an As-terminated surface while growth is interrupted. Substrate temperature is in the 500 °C range. To make the periodically doped multi layer (20 layers), growth is continued until the desired layer spacing is achieved. The cycle is then repeated. Typical inadvertent background doping under the conditions of growth used here is $p$ type, with a concentration of $3\times10^{14}$ acceptors/cm$^3$. This concentration can vary between $1\times10^{14}$ and $6\times10^{14}$ cm$^{-3}$, and is not known precisely.

The choice of the δ-layer density is from the hopping experiments work and theoretical estimates. It was judged to be necessary to have a Si concentration $N_D \approx 1\times10^{11}$ cm$^{-2}$. Earlier work with single layers showed a severe problem with such dilutely doped samples. With the $n$-type δ layer embedded in a buffer and cap materials with unknown background and surface acceptor concentrations, it was not possible to have reproducible δ-layer conduction. The compensation was uncontrolled and so large that the results were erratic and unpredictable. The solution to these problems has been the multiple δ layer.

Figure 1 shows schematically the multilayer sample construction. The design choice for the spacing of the layers was $d = 1000$ Å. for the expected $p$-type background doping of $3\times10^{14}$ cm$^{-3}$, the compensation then would be 3%. Of the 20 layers that make up the structure, we expect the top and bottom layers to be depleted. The conductivity is that of the 18 inner δ layers. All data have been interpreted in this way.

The sample material and its construction is identical with the wafer $A$ mentioned in Ref. 9. The Hall density gives $0.8\times10^{11}$ cm$^{-2}$ electron per sheet when averaged over 18 conducting sheets. We expect this value to have an uncertainty of $\pm0.1\times10^{11}$ cm$^{-2}$. The compensation is estimated to be between 1 and 6%. It is sufficiently small that, in view of the uncertainty in $N_D$, we do not need to distinguish between Si donor density and the number of transport electrons $N_s$. It is known with certainty[5] that the donors are confined to a sheet whose width, if not atomically sharp, is, at most, a small fraction of the average donor spacing of 350 Å.

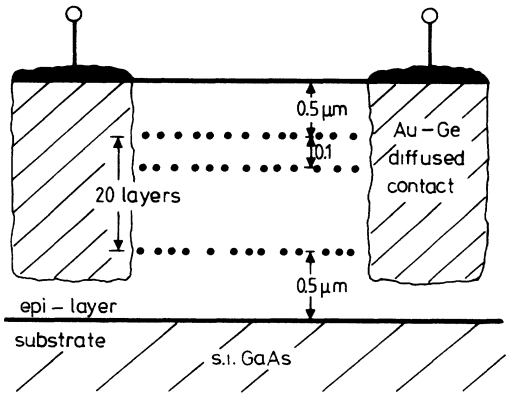


FIG. 1. Schematic drawing of the δ-layer sample designed for the study of transport in the dilute doping limit.

Autocompensation, which occurs when Si donors occupy As sites, is known to be negligibly small for MBE-grown δ layers of the low concentration encountered in the present work. The problem has been studied in local vibrational mode spectroscopy using Raman techniques.[17] MBE growth conditions, in particular the As overpressure during the Si deposition, make impurity incorporation very different from bulk crystal growth where autocompensation may be substantial.

All resistance measurements are made using diffused Au-Ge contacts on a Hall-bar geometry. The lithographically defined sample length is 10 mm, its width is 1 mm. Because of the multilayer construction of the sample it is recognized that the voltage probes short together the various layers. They are thus not free to take on independently the appropriate voltage. In this sense the measurement resembles a two-probe experiment even though it is done with separate current and voltage probes. Nevertheless, the precision and uniformity of MBE growth is a guarantee that the conducting sheets are quite similar. The multilayer construction with sacrificial depleted outer, assures that, in hopping transport, the inner sheets dominate. These are identical within narrow tolerances.

## III. EXPERIMENTAL RESULTS AND DISCUSSION

Having discussed the design of the δ-multilayer system and measurement techniques we turn in this section to experimental observations and their interpretation. There are three different aspects to be considered. We start with an analysis of thermally activated transport in the δ layer in the absence of magnetic field. This is followed by a discussion of magnetotransport in fields parallel and perpendicular to the sample plane. The predominant effect, caused by the compression of the electron wave function, is a positive MR. This effect, together with changes in the activation energy, will be discussed first. There follow data and discussion on the negative MR that results from interference in hopping transport along neighboring alternative paths. All the observations apply to the multilayer sample as described in the previous section. The results are quoted in terms of the resistance per square ($R_\square$) of a single doping layer.

### A. Activated transport for $B = 0$

The variation of the resistance with temperature is shown in Fig. 2. Between 77 and 1.5 K the value $R_\square$ changes by about 3 orders of magnitude, demonstrating that transport is strongly activated. In the temperature range down to 10 K, there is a decrease of the free-carrier concentration. Transport involves the excitation of electrons to the conduction band edge. This process is characterized by an energy $\varepsilon_1$, which is expected to be of the order of the Rydberg energy 5.8 meV.

Below 10 K the resistance rises more slowly with decreasing $T$. This is the regime of hopping transport. The transition rate from site $i$ to site $j$ in thermally assisted

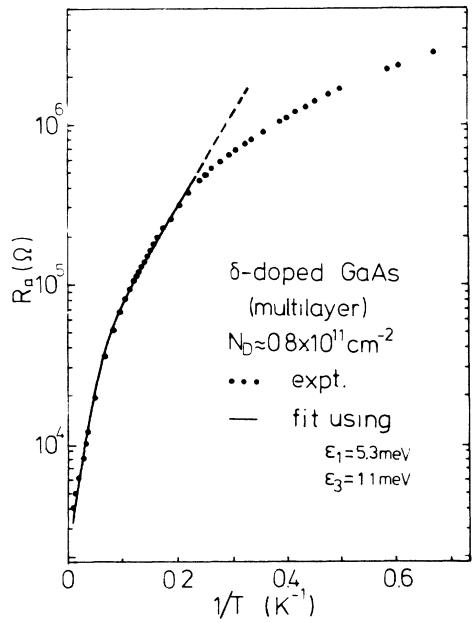


FIG. 2. Sheet resistance ($R_\square$) vs reciprocal temperature for layers contributing to the transport. The solid line models the transport on the basis of excitation to the band edge and nearest-neighbor hopping (NNH). Variable-range hopping (VRH) dominates above 0.2 K$^{-1}$.

hopping is proportional to a factor $\exp(-2r_{ij}/a^*-\varepsilon_3/kT)$, $r_{ij}$ is the distance between the points $i$ and $j$, $a^*$ is the Bohr radius of the impurity state, and $\varepsilon_3$ is the activation energy for impurity-band transport. The term $\exp(-2r_{ij}/a^*)$ is called the site term and is related to the wave-function overlap between sites $i$ and $j$. For the sheet doping density $N_D=0.8\times10^{11}$ cm$^{-2}$, the average spacing between the Si donors of the layer is 350 Å, which is much smaller than the 1000-Å distance between the layers. It follows that hopping in the plane of the layers will exponentially dominate the transport properties in Fig. 2.

Hopping transport distinguishes between two characteristic variants. Nearest-neighbor hopping (NNH) takes place at temperatures high enough such that the contribution of the energy term $\varepsilon_3/kT$ is much smaller than that of the site term. The linear region in the semilogarithmic plot of Fig. 2 between the $1/T$ values 0.1 and 0.2 K$^{-1}$ is typical of NNH. Above 0.2 K$^{-1}$, where $R_\square$ rises more slowly and is curved, the variable-range hopping (VRH) mechanism operates. In this case, restrictions are imposed by the energy term and sites other than nearest neighbors are more favorable. For VRH a distinctly different and dimensionality-dependent power law applies. From the data in Fig. 2 the resistance variation above 0.3 K$^{-1}$ follows approximately the Mott law $R=R_0\exp(T_0/T)^{1/3}$ with $T_0\approx340$ K. The temperature range is too small in order to precisely establish the $T$ dependence of VRH in the present case, and because it is of little importance in this paper, we choose not to pursue this point further at present. What does matter with regard to Fig. 2 is to note that, at temperatures in the 0.2–0.6 K$^{-1}$ range, hopping transport applies. The hopping lengths for the data in Fig. 2 range from the nearest-neighbor distance of 350 Å to somewhat above this in Mott's VRH sense.

The resistance variation in Fig. 2 which describes activation to the mobility edge and NNH, is well fit by summing the parallel conductances in the form

$$(R_\square)^{-1}=[R_1\exp(\varepsilon_1/kT)]^{-1}+[R_3\exp(\varepsilon_3/kT)]^{-1}\ .$$

The solid line passing through the points is obtained for $R_1=2.8$ kΩ, $\varepsilon_1=5.3$ meV, $R_3=28$ kΩ, and $\varepsilon_3=1.1$ meV. In making this fit, the activation energy $\varepsilon_1$ has been taken directly from far-infrared resonance data[18] which measures the electronic excitation energy of the $1s\rightarrow2p$ impurity transition as 4.0±0.2 meV. Scaled according to the expected factor for a hydrogenic impurity, this gives $\varepsilon_1=5.3$ meV. $\varepsilon_1$ is thus not a fit parameter. Its value should be compared with 5.8 meV for isolated impurities.

The value of $\varepsilon_3$ for the finite compensation in the present case relates to Coulomb interactions of dipole pairs. Background acceptors located between the δ layers cause unoccupied sites in the layers and provide a kind of pinning energy. As sketched in Fig. 3, an electron trapped on an acceptor leaves behind a positively charged hole in the δ layer. At low temperature, the holes are bound with an energy that depends on their distance to the nearby negative acceptor site. For small compensation, the hole-acceptor dipole pairs will not influence one another much. To the extent that the hole can be localized as a point charge in the layer, the minimum pinning energy is a term $2e^2/\varepsilon d=2.3$ meV. Here $d$ is the distance between the layers. The largest separation that the hole-acceptor pair can have is $d/2=500$ Å.

The estimate 2.3 meV must be compared to the measured $\varepsilon_3=1.1$ meV. It is easy to see why a smaller $\varepsilon_3$ can be obtained in the experiments. When there is overlap of wave functions in the plane of the δ layer, the hole will not be localized as a point charge. Also, because the

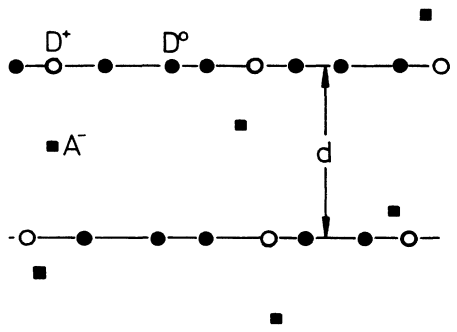


FIG. 3. Schematic drawing of donors ($D$,●) in the δ layer and residual acceptors ($A$,■) distributed throughout the volume. Binding of $D^+A^-$ pairs provides an activation energy $\varepsilon_3$ for the movement of holes in the δ layer.

average spacing in the plane is 350 Å, the net separation of the hole and negative acceptor site is on the average greater than $d/2$. Moreover, for the pinned hole to move by one site, only a fraction of the binding energy is required. The model considered in Fig. 3 provides a reasonable estimate for $\varepsilon_3$ and could serve as a basis for more detailed calculations.

### B. Hopping transport in a magnetic-field magnetoresistance

Experiments in a magnetic field provide additional information on the hopping mechanism, because the field modifies the amplitude and phase of the wave function. For the planar geometry there are three distinct configurations of the field and currents. We refer to the case of field applied perpendicular to the plane of the $\delta$ layer as $B_\perp$. When the magnetic field lies in the plane we need to distinguish current flow parallel and perpendicular to $B_\parallel$. These are labeled, respectively, $B_\parallel^\parallel$ and $B_\parallel^\perp$. Figure 4 shows the magnetic-field dependence of the sheet resistance on a logarithmic scale for each of the three geometries at $T=4.5$ K. The dominant effect seen in that data is a strongly rising resistance which is distinctly different for the $B_\perp$ and $B_\parallel$ configurations. This anisotropy is evidence for the dominant in-plane nature of the hopping transport. For $B_\perp$ there is, in addition, a negative resistance effect. This negative MR will be the subject of the following section. Here we analyze and discuss the positive effect.

Increased resistance is the result of shrinking the wave function both in the plane transverse to the magnetic field and in the longitudinal direction. This compression reduces the exponential tailing and overlap that determines the jump probability between sites. Figure 4 shows that for $B_\perp$ and isotropic wave-function shrinkage in the $\delta$-layer plane, the resistance increases more strongly than for $B_\parallel$. For the latter case, the compression effect is anisotropic in the $\delta$ layer. The longitudinal shrinkage is smaller than the transverse effect. The result is a $B_\parallel$ MR that not only rises more weakly, but also depends on the direction of the current.

To study the influence of the site term for hopping in a magnetic field requires that one first factors out the contribution of the energy term. The data in Fig. 4 contain, in addition to the wave-function shrinkage, the effect of changes of $\varepsilon_3$ with $B$. The activation energy $\varepsilon_3$ can depend on the field for several reasons. Here it is expected to increase because of the increaed localization of the electronic wave function on the donor sites.[1] For the pinning model, discussed in Sec. III A above, increased localization of the hole implies that the positive charge moves closer to the negative acceptor site and becomes bound more strongly. It is expected that changes in $\varepsilon_3$ will differ for $B^\perp$ and $B_\parallel$.

Figures 5 and 6 show $R_\square$ versus reciprocal temperature for various values of $B$ from 0 to 6 T. For the $B_\parallel$ configuration we know from the previous figure that there is a recognizable, but small, difference for the two current directions. Theory shows[19] that the two cases are distinguished by a field-dependent prefactor. The $\perp$-current case has a resistance that rises more steeply by a factor proportional to $B^2$. For the $B$ dependence in the exponential factor (which is expected to be the same for both $\parallel$ and $\perp$ currents), it is therefore necessary to analyze the $B_\parallel^\parallel$ data. For this data in Fig. 5 we proceed to find an $\varepsilon_3$ that best accounts for the variation of $R_\square$ in the range 0.1–0.2 $K^{-1}$, where NNH dominates. The fit leaves the $\varepsilon_1$ value constant. The expected small change in the hydrogenic ground-state energy with $B$ is too small to

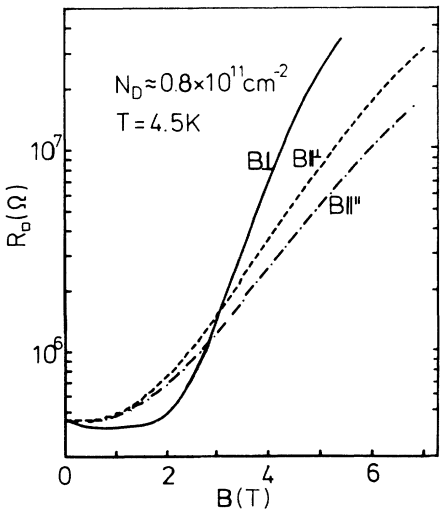


FIG. 4. Magnetic-field dependence of log$R$ measured at 4.5 K. For the parallel $B$ field, two distinct current directions relative to the field are used ($\parallel$ and $\perp$).

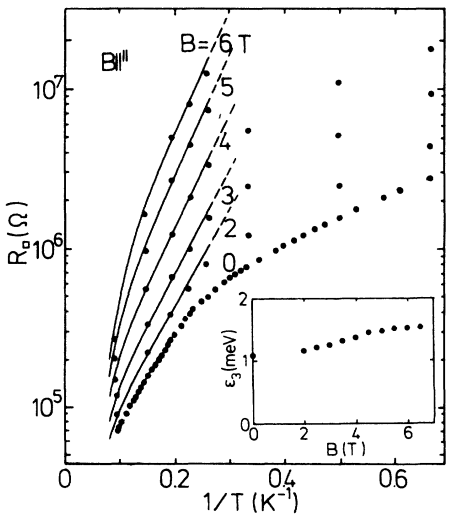


FIG. 5. Sheet resistance $R_\square$ vs reciprocal temperature measured in a different magnetic field with the $B\parallel$ configuration. The solid line is the fit in terms of a fixed $\varepsilon_1$ (5.3 meV) and a $B$-dependent $\varepsilon_3$. The inset shows the magnetic-field dependence of $\varepsilon_3$.

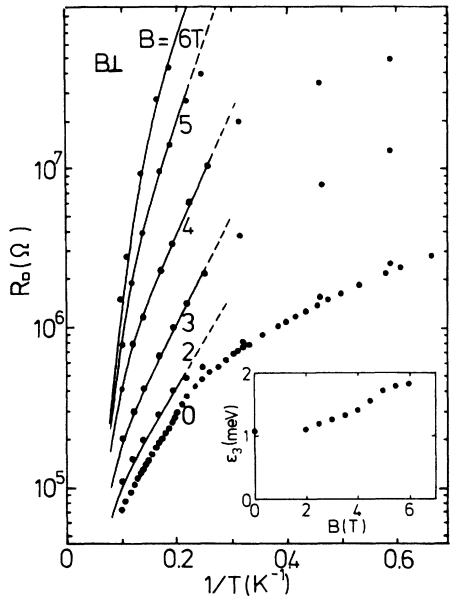


FIG. 6. Sheet resistance $R_\square$ vs reciprocal temperature measured in a different magnetic field with the $B_\perp$ configuration. The solid line is the fit in terms of a fixed $\varepsilon_1$ (5.3 meV) and a $B$-dependent $\varepsilon_3$. The inset shows the magnetic-field dependence of $\varepsilon_3$.

significantly change the $\varepsilon_3$ result. The variation of $\varepsilon_3$ with $B$ is given in the inset.

Working with the $B_\perp$ data in Fig. 5 is complicated by the negative-MR effect. To get the $\varepsilon_3$ versus $B$ in this case we have ignored the data below 2 T where the decreasing resistance dominates. In making the fits we follow the procedure for the previous case. $\varepsilon_1$ is left constant at 5.3 meV. The $\varepsilon_3$ versus $B$ in both cases are reasonable and can be accounted for qualitatively in terms of the pinning-energy description. The magnetic field reduces the overlap of the hydrogenic states in the δ layer. This, in turn, leads to an increased localization of the hole in the δ layer. It becomes more like the point particle used to estimate the 2.3-meV energy. It follows that the measured value of 1.1 meV should rise. Since, for $B_\parallel$, the wave-function compression in the plane of the δ layer is smaller, one should expect the $\varepsilon_3$ versus $B_\parallel$ to rise more slowly.

Having available $\varepsilon_3$ versus $B$, we can return to data such as in Fig. 4 in order to extract the magnetic-field dependence of the site term. For three-dimensional case the theory is worked out in Ref. 1. We cite here the main results and restrict the discussion to the NNH regime. For small $B$, the range of the exponentially decaying ground-state wave function is decreased by a term proportional to $B^2$. The expected increase of resistance is predicted to be an expression of the form $R_\square(B) = R_0 \exp(\Delta B^2)$, where $\Delta$ is a geometry-dependent factor $(\perp, \parallel)$. In the two-dimensional case, the magnetoresistance follow a similar expression. Using percolation calculations, $\Delta$ has been evaluated by different authors. For the perpendicular case Nguyen[20] obtains

$$\Delta_\perp = 0.143 a^* e^2/(N_D^{3/2} h^2) .$$

For parallel fields the factor as calculated by Xia *et al.*[16] is independent of the current direction and has exactly one-half the numerical value, i.e., $\Delta_\parallel = 0.5\Delta_\perp$. The current direction ($\perp$ or $\parallel$) does not enter in the derivation of the exponential.

To obtain experimental values for $\Delta_\parallel$ from the MR curves, we first factor out the part of the resistance coming from $\varepsilon_3(B)$. For the parallel field geometry, we make use of the $B_\parallel$ data and fit to a parabolic variation from 0–4 T. This fit has been made at various temperatures in the NNH range. The results for $\Delta_\parallel$ are entered in Fig. 7. For the perpendicular MR it is necessary to identify the part of the resistance variation caused by the negative MR. This is done by fitting the slope in a $B^2$ plot only above 2 T, where the negative contribution appears negligible (cf. Fig. 4). In this way the values of $\Delta_\parallel$ and $\Delta_\perp$ plotted in Fig. 7 have been obtained. Both $\Delta$ values are nearly constant with $1/T$ and they have a ratio close to the predicted 0.5. The independence of temperature is an important test, relating to the proper identification of $\varepsilon_3(B)$.

Additional confirmation of the analysis comes from comparing the value of $\Delta_\perp$ from experiment and theory. When we average over the various $1/T$ points, we have $\Delta_\perp = 0.12$ from Fig. 7. Theory gives $\Delta_\perp$ in terms of known constants, with $N_D$ being the only experimental parameter. Substituting for $a^*$ (100 Å) and the other quantities in the expression given earlier for $\Delta_\perp$ allows us to solve for $N_D$. This is the $N_D$ that theory predicts for the measured $\Delta_\perp = 0.12$ T$^{-2}$. Its value is $N_D = 0.9 \times 10^{11}$ cm$^{-2}$. The experimental value is $0.8 \times 10^{11}$ cm$^{-2}$. Because the Hall measurement gives only $N_D$-$N_A$ because of the finite compensation, it is expected that the theory number is somewhat greater. Considering that there are no adjustable parameters, this agreement must be considered as substantial evidence for a proper description.

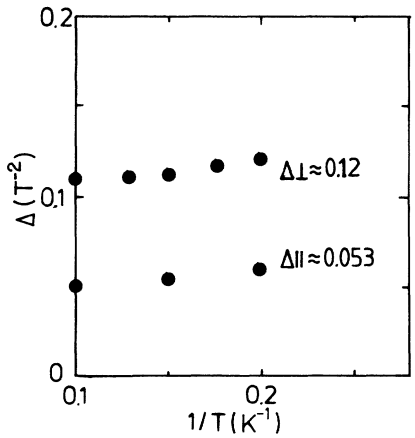


FIG. 7. Values of the factor $\Delta$ in the exponential field dependence of resistance due to the site term in hopping, i.e., $R(B) = R_\square \exp(\Delta B^2)$. Temperature independence proves the internal consistency of the analysis.

### C. Negative magnetoresistance

The most fascinating experimental result is the observation of the distinct and sizable negative MR in the $B_\perp$ configuration (Fig. 4). In order to study this interesting physical phenomenon, we show in Fig. 8 the MR traces measured at three temperatures on an enlarged scale. For the $B_\perp$ configuration the negative-MR effect dominates over a wide magnetic-field range. For $B > 1.5$ T, the positive MR takes over. For the $B_\parallel$ configurations, there is a much weaker negative MR at the low-$B$ field.

The negative MR is related to the phenomenon first discussed by Nguyen *et al.*[10] These authors pointed out that because of the long-range hops contributing to the VRH conduction, the scattering of tunneling electrons by intermediate donors is important. Some scatterers can change the sign of the scattered wave. As a result, destructive interference by alternative paths from initial to final states arises. For the extreme case the total probability of a hop is close to zero because of the cancellation of amplitudes of different paths. The applied magnetic field gives rise to an orbital factor $\exp(i\phi)$ for each pair of paths, where $\phi$ is the magnetic phase factor $\phi = 2\pi BS\cos\theta/\Phi_0$. $\Phi_0 = h/e$ is the quantum flux unit, $S$ is the area bounded by the alternative paths connecting the initial and final state of the hop. $\theta$ is the angle between the normal of the area and the magnetic-field direction. The phase factors make small values of the hop probability unlikely and thus increase the conductivity. The simplest estimate for the typical area $S_0$ is $S_0 = r^{3/2}/(a^*)^{1/2}$, where $r$ is the mean hopping distance. Thus, the typical magnetic phase factor is $\phi_0 = 2\pi BS_0/\Phi_0$.

Nguyen *et al.*[10] have shown that for small magnetic fields, where $\phi_0 < 1$,, the MR is negative and grows linearly with $B$. Sivan *et al.*[11] and Entin-Wohlman *et al.*[21] have found that in a certain small-field region the linear $B$ dependence should be replaced by a $B^2$ relation. A comprehensive discussion of the field dependence of the negative MR is given by Entin-Wohlman *et al.*[21] and Shklovskii and Spivak.[22] Recently Schirmacher[15] proposed a simpler, physically intuitive model for this interference of different paths (Fig. 9). In this model only a single scattering event, changing the sign of the wave function, is involved. This model is particularly suited for the transtion region from NNH to VRH where scattering by many donors is unlikely. When there are only two contributions to $\psi$ in the final state

$$\psi = \psi_1 + \psi_2 \exp(i\phi) ,$$

where $\psi_1$ is due to the straight path and $\psi_2$ is due to the path which involves one scattering event.

Keeping Fig. 9 in mind, let us now discuss the experimental data. Except for the region of extremely small fields where the MR is positive, the negative MR dominates. As shown in Fig. 8, with decreasing temperature, the negative-MR magnitude becomes stronger. At 4.5 K the maximum of $\Delta R/R$ is of order 10%. It increases to over 25% at 1 K. Since the magnetic field where the $\Delta R/R$ has its maximum changes with temperature, we cannot use the magnitude to study the temperature dependence of the negative-MR effect. Instead, we note that over the field range up to 0.5 T, the $\Delta R/R$ is approximately linear in $B$. This agrees with the predictions by Nguyen *et al.*[10] and Schirmacher.[15] The linear dependence suggests using the slope $\gamma \equiv d(\Delta R/R)/dB$ as a measure of the magnitude of the negative-MR effect. $\gamma$ can be calculated explicitly.[15]

We evaluate the slope $\gamma$ as marked in Fig. 9 for both the $\perp$ and $\parallel$ configurations. For the $\parallel$ case it is difficult to extract the purely negative-MR contribution to the slope because its magnitude is so small. We note in Fig. 8 that at low field the $B_\parallel$ curves lie above the $B_\parallel^\perp$ data. They are seen to cross at higher field. In Fig. 10 we plot the $\ln\tau$ versus $\ln T$ for both orientations of the magnetic field. $\gamma$

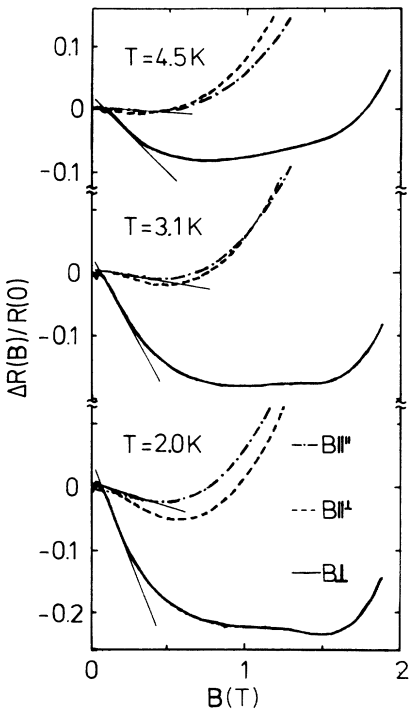


FIG. 8. Relative magnetoresistance $\Delta R(B)/R(0)$ as function of the magnetic field for the three configurations at various temperatures. The thin solid lines at low field indicate that the $\Delta R/R$ is linear in the $B$ field.

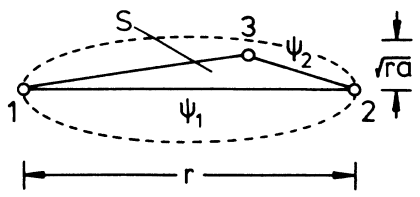


FIG. 9. Schirmacher's triangle showing the areas generated by the direct and one alternative path between points 1 and 2.

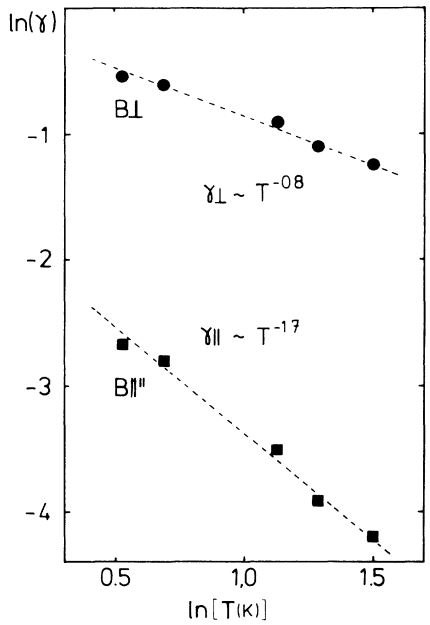


FIG. 10. Dependence of $\ln(\gamma)$ on $\ln(T)$ for the two orientations of the magnetic field. $\gamma[\equiv d(\Delta R/R)/dB]$.

is increases according to a power law. For the perpendicular case $\gamma_\perp \propto T^{-0.8}$, for the parallel geometry $\gamma_\parallel \propto T^{-1.7}$. The parallel case has a considerable uncertainty because of the overlapping positive MR. What matters here is to note that the variation would be even steeper if a background MR were subtracted. For the perpendicular geometry, the physical origin for the dependence of $\gamma$ on temperature is clear. In terms of the model, with decreasing $T$, the hopping distance, and thus the area $S$ bounded by different paths, increases. The magnetic field necessary to destroy the coherence becomes less. It follows that the resistance will decrease more quickly with $B$.

We next examine the negative MR for the $B_\parallel$ case. If all the donors were located precisely in the plane of the δ layer, there should be no negative MR for this configuration. The magnetic phase factor $\phi$ is strictly zero. We indeed find a strong anisotropy. $\gamma_\parallel$ is smaller than $\gamma_\perp$ by a factor of 20 at $T=4.5$ K and by factor of 9 at $T=1.7$ K. Nevertheless, we still have to explain why it is finite. We suggest that $\gamma_\parallel$ is finite because there is a small background concentration of dopants in the bulk of the sample. Bulk dopants give rise to a small, but finite, number of hops with nonzero phase factor $\phi$. This hypothesis is supported by the temperature dependence of $\gamma_\parallel$ and $\gamma_\perp$. With decreasing temperature, $\gamma_\parallel$ increases significantly faster than $\gamma_\perp$. If the negative MR for $B_\parallel$ were caused by the scattering from bulk dopants, then the effect of negative MR would be characterized by the volume $V \approx r^2 a^*$.[10] For the $B_\perp$ configuration, the effect was linked with the area $S \approx r^{3/2}(a^*)^{1/2}$, since most scatterers lie in the δ layer. When $r$ increases with decreasing temperature, the volume increases as $r^2$, while the area $S$ increases only as $r^{3/2}$. It follows that negative MR for $B_\parallel$ has a stronger $T$ dependence than that for $B_\perp$. At very low temperature, when the hopping distance $r$ exceeds the interlayer spacing $d$ in the sample, the anisotropy of the negative MR must disappear.

One can propose yet another model of the $B_\parallel$ effect. Assuming that the δ layer has a finite thickness $z$, then the effect of the negative MR for $B_\parallel$ is characterized by the area $S \approx rz$. With the increase of $r$, the anisotropy of $\gamma$ will increase. Such an increase of the anisotropy with decreasing temperature was indeed observed in Ref. 13 where thin $In_2O_3$ films, which resemble a 2D system with finite width, were investigated. The decreasing anisotropy in our experiments confirms the first model of sharply doped layers with small background. The negative MR thus provides an indication of the finite donor spreading or the existence of background dopants.

We return to Fig. 8 to discuss the saturation of the negative-MR effect. For the highest temperature, the effect of the negative MR saturates near $B=0.7$ T. With decreasing temperature, the effect of the negative MR extends to higher field. The $T=2$ K curve has a minimum near $B=1.5$ T. We attribute this change to the change of the scattering mechanism. As noted in Sec. III A, the transition region from NNH to VRH occurs for $T=5$ K. The negative MR in this temperature range mainly comes from the interference of alternative paths involving a single scattering event, as described by Schirmacher's triangle model.[15] With decreasing temperature, multiple scattering becomes more and more important. This causes the negative MR to persist to higher field. A detailed theoretical analysis of the negative MR involving multiple-scattering events is planned. It also remains to account for the additional structure at very low fields, as well as for the hump near 1 T, that appears in Fig. 8 at the lowest $T$.

## IV. CONCLUDING REMARKS

We have demonstrated in the present experiments that the dilutely doped δ-multilayer system provides an interesting new 2D system on which to study hopping transport. In contrast to other layered structures such as $Na^+$-ion-doped MOS interfaces, the Ge-bicrystal interface, or amorphous $In_2O_3$, the δ layer is a near-perfect semiconductor fabricated with MBE precision according to design. We remind the reader that the multilayer aspect is an essential part of that design and that it has helped us control the compensation effects of background acceptors and boundary sufaces.

The work here has a concentrated effect on the NNH regime. The known Coulombic potentials, the quantitative precision of doping with regard to densities and position, and the fact that the experiments could be done in an easily accessible range of fields and temperature has made it possible to provide quantitative measures of physical quantities related to hopping transport.

Comparing what has been achieved in the work on positive MR for Ge bicrystals,[16] we note that our work has

provided a donor density that can be compared directly with the design doping. We have found that $\varepsilon_3$ versus $B$ rises and have given reasons for this increase. We have used the $\varepsilon_3$ versus $B$ in order to derive the data of the purely magnetic-field-induced wave-function shrinkage effect. The factor was found to be independent of temperature. This is an indication of internal consistency.

The strong and anisotropic negative MR provides experimental evidence for the quantum-interference effect in the VRH regime in a two-dimensional system. From the changes of the anisotropy of the negative MR with temperature, we get information about the finite donor spreading and the existence of background dopants. There are some loose ends, things for which we have only given qualitative explanations and arguments. It also remains to do a more complete $T$ dependence for VRH. In future work $\delta$ layers in other materials or with different density or degree of compensation should be studied.

## ACKNOWLEDGMENTS

We thank W. Schirmacher for the close cooperation and the many discussions that have led to a better understanding of the experimental observations. These, in turn, have initiated and motivated his theoretical work. A. Zrenner thanks Siemens A.G. for financial support. The work was sponsored by the Deutsche Forschungsgemeinschaft (Bonn, Germany). Samples were grown with the support of the Bundesministerium für Forschung und Technologie (Bonn, Germany).

*Permanent address: A. F. Ioffe Physico-Technical Institute, Academy of Sciences of U.S.S.R., 194021 Leningrad, U.S.S.R.

[1]B. I. Shklovskii and A. L. Efros, *Electronic Properties of Doped Semiconductors,* Vol. 45 of *Springer Series in Solid-State Sciences* (Springer, Berlin, 1984).

[2]G. Timp and A. B. Fowler, Phys. Rev. B **33**, 4392 (1986).

[3]J. L. Robert, A. Raymond, J. Y. Mulot, and C. Bousequet, *Gallium Arsenide and and Related compounds, 1987,* Inst. Phys. Conf. Ser. No. 91 (IOP, Bristol, 1987), p. 585.

[4]A. Zrenner, H. Reisinger, F. Koch, and K. Ploog, in *Proceedings of the 17th International Conference on Physics and Semiconductors,* San Francsco, 1984, edited by J. D. Chadi and W. A. Harrison (Springer, Berlin, 1985), p. 325.

[5]A. Zrenner, F. Koch, and K. Ploog, Surf. Sci. **196**, 671 (1988).

[6]F. Koch and A. Zrenner, Mater. Sci. Eng. **B1**, 221 (1989).

[7]K. Ploog, M. Hauser, and A. Fischer, Appl. Phys. **A45**, 233 (1988).

[8]A. Zrenner, F. Koch, J. Leotin, M. Goiran, and K. Ploog, Semicond. Sci. Technol. **3**, 1132 (1988).

[9]Qiu-yi Ye, A. Zrenner, F. Koch, and K. Ploog, Semicond. Sci. Technol. **4**, 500 (1989).

[10]V. L. Ngyuen, B. Z. Spivak, and B. I. Shklovskii, Zh. Eskp. Teor. Fiz. **89**, 1770 (1985) [Sov. Phys.—JETP **62**, 1021 (1986)].

[11]U. Sivan, O. Entin-Wohlman, and Y. Imry, Phys. Rev. Lett. **66**, 1566 (1988).

[12]A. Hartstein, A. B. Fowler, and K. C. Woo, Physica B+C (Amsterdam) **117B+118B**, 665 (1983).

[13]O. Faran and Z. Ovadyahu, Phys. Rev. B **38**, 5457 (1988).

[14]E. I. Laiko, A. O. Orlov, A. K. Savchenko, E. A. Ilyichev, and E. A. Poltoratsky, Zh. Eksp. Teor. Fiz. **93**, 2204 [Sov. Phys.—JETP **66**, 1264 (1987)].

[15]W. Schirmacher, Phys. Rev. B (to be published).

[16]Yi-ben Xia, E.Bangert, and G. Landwehr, Phys. Status Solidi B **144**, 601 (1987).

[17]J. Wagner, M. Ramsteiner, W. Stoltz, M. Hauser, and K. Ploog, Appl. Phys. Lett. (to be published).

[18]Qiu-yi Ye, Doctoral thesis, Technical University of Munich, 1989.

[19]See, for example, B. I. Shklovskii and A. L. Efros, *Electronic Properties of Doped Semiconductors,* Ref. 1, pp. 168–189.

[20]V. L. Nguyen, Fiz. Tekh. Poluprovodn. **18**, 335 (1984) [Sov. Phys.—Semicond. **18**, 207 (1984)].

[21]O. Entin-Wholman, U. Sivan, and Y. Imry (unpublished).

[22]B. I. Shkloviskii and B. Z. Spivak, in *Hopping Conduction in Semiconductors,* edited by M. Pollak and B. I. Shklovskii (North-Holland, Amsterdam, 1989).